# Overlay Mark Design Using Irregular Grating Patterns

Hyun-Chul Lee [a], Hyun-Jin Chang [a], Ho-Sung Woo [b,*]

[a] *Auros technology, 5-23, Dongtansandan 6-gil Dongtan-myeon KR, Hwaseong-si, Gyeonggi-do, 18487, Republic of Korea*
[b] *Department of EduTech, Graduate School, Korea National Open University, Seoul 03087, Republic of Korea*
*Corresponding author: [*]hughwoo@knou.ac.kr*

*Abstract*— **Overlay refers to controlling the vertical alignment and misalignment between circuit patterns manufactured in the previous process and circuit patterns manufactured in the current process during the stacking process of circuit patterns in the semiconductor manufacturing process. A critical factor in ensuring precise overlay measurements is using an optimized overlay mark design. Many semiconductor manufacturers have put considerable effort into optimizing overlay measurement marks to reduce high costs. However, image-based overlay measurement encounters several challenges, including resolution degradation, image distortion, and noise introduction during digital data conversion. These issues can amplify the uncertainty of overlay measurements, impair optical resolution, and heighten the risk of mismeasurement. In this paper, we introduce irregular grating patterns designed to address the principal challenges faced by the commonly utilized Advanced Imaging Metrology (AIM) marks, namely large overlays and image distortion. Furthermore, we propose an overlay mark capable of precisely identifying overlays exceeding half a pitch and incorporating as much data as possible within the limits of optical resolution. This aims to improve overlay measurement performance. The experimental findings demonstrate that the proposed Pulsated Grating Target (PGT) mark enhances overall measurement uncertainty by approximately 17% compared to the AIM mark. The practical applicability of the PGT was validated through experiments, and we achieved enhanced precision and reliability in overlay measurements by resolving the issue of large overlays—the most significant challenge with grating patterns—and simultaneously enhancing mark performance.**

*Keywords*— **Semiconductor; overlay metrology; overlay marks; grid patterns; optical resolution.**

## I. INTRODUCTION

Overlay metrology is crucial for controlling the vertical alignment between circuit patterns fabricated in successive processes during the stacking of circuit patterns in the semiconductor manufacturing process [1]–[5]. The vertical alignment is commonly referred to as the overlay, a numerical value that is quantified to verify that the patterns are accurately aligned in the photolithography process [6]. The main techniques for detecting circuit patterns include image processing-based techniques [7], [8], phase diffraction grating-based techniques [9]–[12], and laser interference-based techniques [13]. Among these, image processing-based overlay control is the predominant method used for wafer alignment in lithographic tools, favored for its simplicity and intuitive process [14]. However, the pixel size of digital images obtained via optical systems falls within the micron range, presenting challenges in meeting the overlay accuracy requirements. Consequently, image-based measurement methods employ an optimized, dedicated overlay mark to

attain higher accuracy and resolution [15], [16]. The overlay mark, designed to be larger than the lithographed device pattern on the wafer, is segmented into various layers, featuring patterns in both the X- and Y-axis directions for each layer. Typically, the patterns of the top and bottom layers are crafted to have matching centers of symmetry, with the overlay value determined by the disparity between these centers. Overlay discrepancies may arise from defects such as disconnections or short circuits between patterns, which can occur inadvertently or due to the optical system's influence. An optimized overlay mark design is critical in ensuring precise measurement [17].

Owing to the significant cost associated with semiconductor manufacturing, considerable effort has been dedicated to optimizing overlay metrology within the manufacturing process. However, this process is prone to various issues, including resolution degradation, image distortion, and noise insertion during the conversion to digital data. These challenges can heighten the uncertainty of overlay measurement, impair optical resolution, and elevate the risk

of mismeasurement. Specific design directions for conventional overlay marks have been proposed [1], [18].

First, creating patterns resistant to the manufacturing process has been suggested. Numerous processes occur on the wafer, necessitating the design of patterns to be as simple as possible to minimize the likelihood of these processes inducing defects in the overlay patterns. Thus, conventional patterns are crafted as straightforward, elongated bar shapes to achieve resilience against various processes.

Second, incorporating as much information as possible within a constrained space has been advocated. Although the overlay mark is placed within the scribe lane on the wafer, the available area is limited. Given this spatial constraint, a mark design that maximizes informational content is essential. The volume of pattern information necessary for accurate measurement enhances iterative reproducibility. Consequently, conventional overlay patterns employ periodic grating patterns to optimize the insertion of pattern information within the limited space available.

Considering these design directions for more accurate overlay measurement, it is essential to periodically incorporate a pattern with a bar as long as possible or to design an optimized mark. Despite these considerations, marks employing conventional periodic grating patterns encounter a significant overlay issue. This large overlay problem refers to a phenomenon in which incorrect overlay measurement of one pitch occurs through correlation analysis [19] when an error exceeding half a pitch arises due to the periodicity of a signal acquired for measurement.
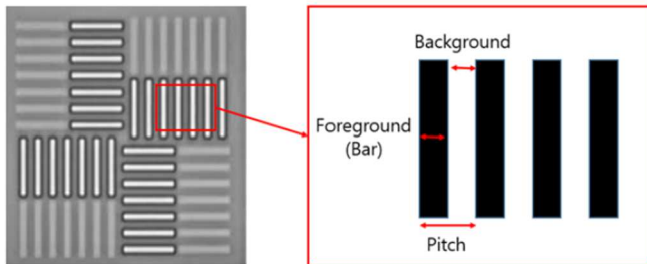


Fig. 1  Advanced imaging metrology (AIM) mark (grating pattern)

Fig. 1 shows the advanced imaging metrology (AIM) mark, currently the most commonly used overlay marker. The AIM mark employs a grating pattern characterized by regularly spaced bars against the background, which maximizes data information within a constrained space [20]–[22]. A bar and the background merge to establish a regular cycle called the pitch. In the design of a grating pattern, the dimensions of the bar and the background must be tailored to the specific objective. Furthermore, given the limited space for inserting the measurement pattern, it should be designed to efficiently accommodate as many bars as possible.

As the density of the bars within a limited space increases, the strength of the signal diminishes. Beyond a certain threshold of signal strength, further improvements in measurement precision are not observed; hence, it is beneficial to augment the density while preserving the minimum signal strength required. Consequently, a recent trend in design involves creating overlay marks that decrease the pitch and enhance the pattern's density. Nevertheless, increasing data density also elevates the risk of large overlays, representing a limitation of conventional grating patterns.

Another issue encountered is image distortion. Image-based overlay measurement employs a refractive optical system comprising lenses and a light source that illuminates the overlay mark with a broad wavelength band of light. In this scenario, the captured image of the overlay mark is invariably distorted due to chromatic aberration, which arises from the variation in refractive indices across different wavelengths of the light source, and spherical aberration, which occurs based on the lens position through which the light is transmitted. Specifically, in the case of the AIM mark, bars progressively farther from the center are inserted sequentially, leading to a disparity between the bars near the center and those further from the center.

This study introduces an irregular grating pattern designed to address the significant challenges of large overlay and image distortion associated with the commonly used AIM mark. Furthermore, we propose an enhanced overlay mark design utilizing this pattern, which aids in detecting overlays exceeding half a pitch. Additionally, this study aims to augment overlay measurement performance by maximizing data insertion within the constraints of optical resolution and optimizing pattern positioning. Ultimately, the structure of this paper is organized as follows: Section 2 details the process of addressing the issues through the proposed method. Section 3 validates the approach through experimental verification, and Section 4 presents the conclusion.

## II. Materials and Method

### A. Proposed Irregular Grating Pattern

The pitch spacing increases or decreases from the pattern's center in the irregular grating structure proposed in this study. This configuration enables the resolution of mismeasurements involving large overlays exceeding half the pitch spacing while simultaneously maintaining signal strength and enhancing the density of the bars compared to conventional grating patterns. There has recently been a trend toward augmenting the number of bars in the overlay mark to improve the precision performance of measurement equipment. However, increasing the number of bars also raises the likelihood of encountering significant overlay issues, necessitating precise control.

Furthermore, edge blur increases the likelihood of encountering significant overlay issues in high-order layers. The proposed irregular grating pattern can incorporate more bars than conventional grid patterns in a high-order layer environment, making it an effective solution for utilizing space when a small overlay mark is necessary. Fig. 2 (a) shows a conventional grating pattern, while Fig. 2 (b) shows the proposed irregular grating pattern. In the case of the irregular grating pattern, unlike the conventional grating pattern, the periodic patterns' pitches are set differently to form an aperiodic overall pattern signal, as shown in Fig. 2(b). A correlation-based measurement algorithm on this foundation addresses the significant overlay problem, characterized by misalignments exceeding one pitch. The irregular grating pattern offers a strategy for preserving signal strength while enhancing the density of the measurement data. An increase in density implies that more bars can be accommodated within the same area than possible. The

quantity of bars and signal strength are critical aspects that can elevate measurement precision [18].
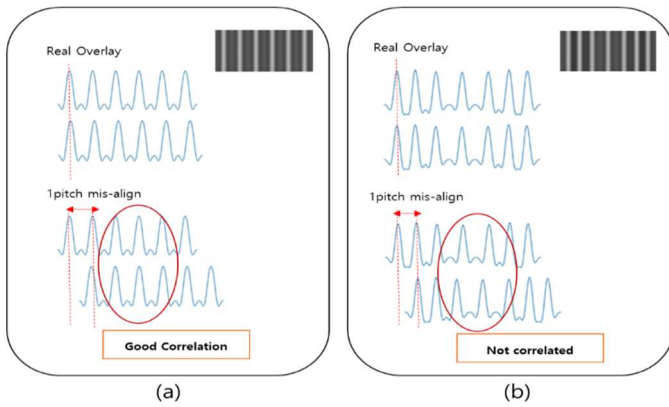


Fig. 2 Large overlay problem

Fig. 3 shows the result of measuring the pattern signal by altering the background. Due to the influence of the color filter, the background appears bright, and the bars appear dark. In this scenario, the signal from the background in the center is elevated. However, signal strength around the outer boundary is diminished, potentially negatively impacting the measurement.
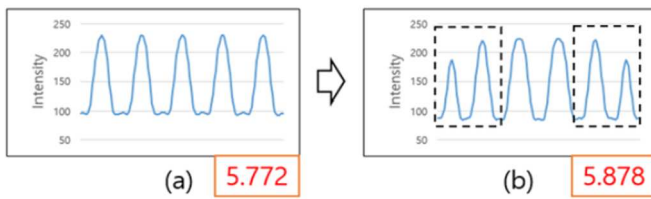


Fig. 3 Comparison of signal strength and density between grating patterns (typical signals): (a) regular grating, (b) irregular Grating
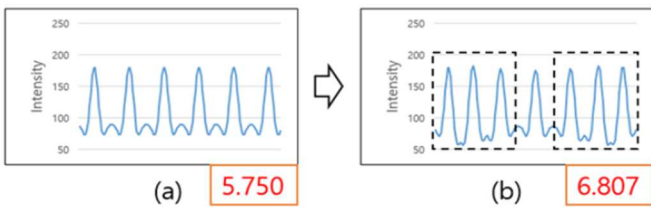


Fig. 4 Comparison of signal strength and density between grating patterns (with signal inversion effect): (a) regular grating, (b) irregular Grating

Nevertheless, if the wavelength and focus are adjusted using the same irregular grating pattern to reverse the signal, the weakened signals around the outer boundary can be enhanced. Consequently, a pattern with enhanced signal strength and density within the identical area can be achieved by employing the irregular grating pattern and reversing the signal, as demonstrated in Figure 4.

*B. Proposed Pulsated Grating Target (PGT)*

In this study, we propose a PGT, a novel overlay mark that leverages the benefits of irregular grating patterns. The PGT is designed to enhance the accuracy and precision of measurements by utilizing irregular grating. The PGT aims to offer an overlay mark capable of minimizing signal degradation attributed to focal error and process effects. This objective is achieved by varying the spacing between the bars and altering the signal density. A vital advantage of this approach is the ability to increase the density of the bars to boost the signal, as the contrast between the maximum and minimum signal values remains relatively high even with reduced spacing between the bars. This benefit is particularly significant in the development of more minor marks. Because patterns with the exact center coordinates are formed in different processes, the overlay measurement can be performed by comparing the center position between the two patterns [23]–[25].
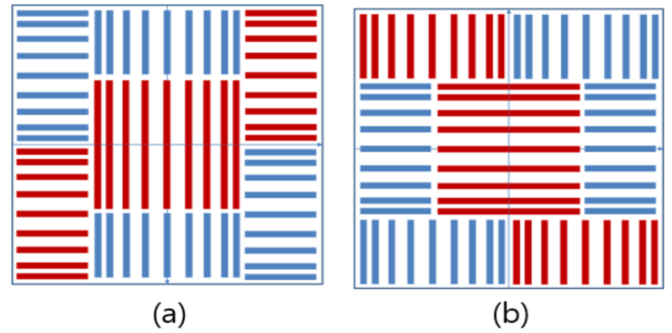


Fig. 5 Pulsated grating target (PGT) design: (a) vertical PGT, (b) horizontal PGT

Fig. 5 shows two PGT designs. The position of the PGT pattern is designed by placing a specific directional pattern in the center, considering the optical aberration directionality. Considering the lithography scan direction, this can minimize the wafer-induced error (WIS) [26], [27]. The effect of optical components, such as the beam splitter, and the light path difference occurring in a specific direction was minimized by positioning a pattern with a high susceptibility to aberration at the center of the overlay mark. This design approach aims to reduce the influence of aberration contingent on the lithography scan direction. Figure 5 illustrates designs that effectively minimize aberration effects in both horizontal and vertical directions.

The bars placed in one direction (X- or Y-axis direction) were put together in the center. When capturing the image of the overlay mark, it was essential to position the overlay measuring device such that the beam splitter (BS) [28], an inclined optical element, aligns with the axis (X- or Y-axis) corresponding to that direction. This alignment minimizes the effect of optical aberration. Fig. 6(a) shows the inclined optical element, while Fig. 6(b) shows the process of acquiring the overlay mark through the scanner.
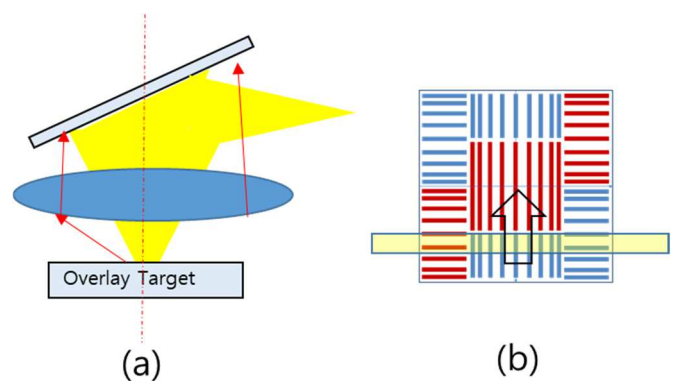


Fig. 6 Minimization of the influence of optical aberrations: (a) inclined optical elements, (b) process for acquiring the overlay mark through a scanner

In the overlay mark detection step, the scan direction of the lithography device is set in the same direction as the bar length direction (Y-axis direction) of the pattern placed in the center. As constant speed control can be performed in the scan direction of the lithography device, the distortion in the Y-axis direction of the bars is not significant. However, as distortion may occur in the X-axis direction, the bars aligned with the X-axis direction perpendicular to the scan direction can be placed in the center to minimize the distortion, which is desirable.
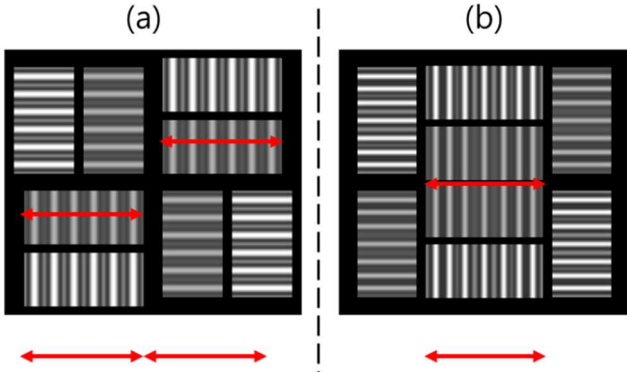


Fig. 7 Minimizing the impact of optical aberrations due to differences in distance from the inclined optical elements: (a) conventional overlay mark (AIM), (b) proposed overlay mark (PGT)

As shown in Fig. 7, when the total area of the proposed overlay mark (Fig. 7b) is the same as that of the conventional overlay mark (Fig. 7a), the distance between the bars placed at both ends in the X-axis direction of the traditional mark of overlay (the width of the X-axis direction of the overlay mark) is relatively shorter than that of the conventional overlay mark. Consequently, the variance in the distance in the Z-axis direction between the bars at both ends and the BS, an inclined optical element, is less than that observed in the conventional overlay mark. This configuration implies that the impact of optical aberration, resulting from the distance difference to the inclined optical element, can be minimized.

## III. RESULTS AND DISCUSSION

### A. AIM vs. PGT Simulation Test

Experiments and tests were conducted using two approaches to verify the target: simulations and utilizing actual devices with test wafers. For the simulations, the RSoft tool (Synopsis, Inc.) employing the rigorous coupled-wave analysis (RCWA) algorithm was used to evaluate measurability and performance. The input variables for the RSoft tool are categorized into simulation structure (stacked structure, lattice structure, structural analysis domain), material information (e.g., refractive index), and incident light characteristics (wavelength, angle, polarization). The simulation structure was designed to represent an arbitrary structure, as depicted in Fig. 8.

Fig. 8 presents the cross-sectional details of the test structure within the simulation environment. The applied wavelength during the simulation ranged from 450 to 750 nm (bandwidth of 300 nm), with the Numerical Aperture (NA) condition set to input NA 0.3 and output NA 0.7 for conducting the test. The comparative analysis employed the IBO AIM mark and IBO PGT mark. The IBO AIM mark was

designed with a pitch of 2 μm and a line width of 0.8 μm, while the IBO PGT mark configurations included pitches of 1.4, 1.6, 2.0, 1.6, or 1.4 μm and a line width of 0.8 μm.



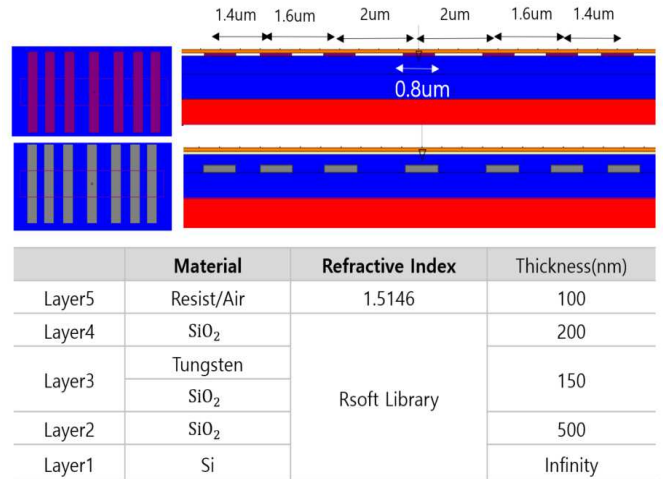| | Material | Refractive Index | Thickness(nm) |
|---|---|---|---|
| Layer5 | Resist/Air | 1.5146 | 100 |
| Layer4 | SiO₂ | | 200 |
| Layer3 | Tungsten | Rsoft Library | 150 |
| | SiO₂ | | |
| Layer2 | SiO₂ | | 500 |
| Layer1 | Si | | Infinity |

Fig. 8 Simulation environment

Fig. 9 and Fig. 10 show the evaluation results of the AIM and PGT marks based on the RCWA simulation results. For this simulation evaluation, the current layer of the AIM and PGT marks was held constant, while the previous layer was artificially shifted to derive the results. Utilizing the existing pattern for each case, we calculated the kernel's center of gravity (CoG) and measured the overlay between the two layers [29].
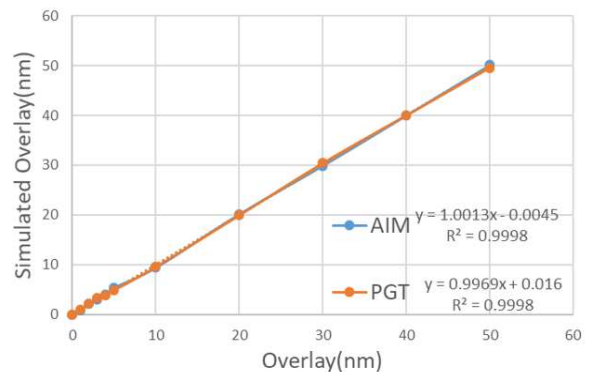


| OVL(nm) | AIM | PGT |
|---|---|---|
| 0 | 0.03336 | 0 |
| 1 | 0.88008 | 1.02512 |
| 2 | 2.08248 | 2.12992 |
| 3 | 3.05344 | 3.2596 |
| 4 | 4.06 | 3.93312 |
| 5 | 5.3708 | 4.84984 |
| 10 | 9.40304 | 9.54656 |
| 20 | 20.18376 | 19.92336 |
| 30 | 29.9012 | 30.41744 |
| 40 | 40.03176 | 40.00376 |
| 50 | 50.15992 | 49.5744 |
| Slope | 1.001 | 0.997 |
| R2 | 1.000 | 1.000 |

Overlay Range : 0~50nm

Fig. 9 Matching performance analysis of AIM and PGT: Overlay Range 0~50nm
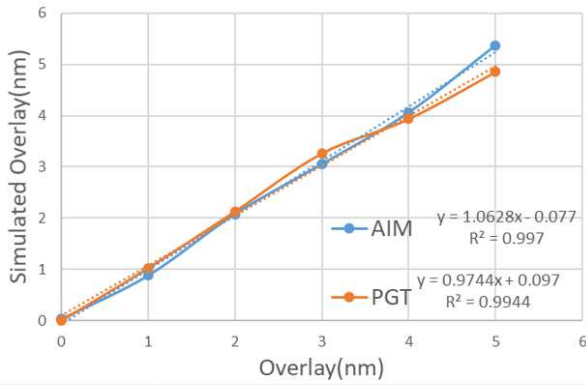
Fig. 10 Matching performance analysis of AIM and PGT: Overlay Range 0~5nm

| OVL(nm) | AIM | PGT |
|---|---|---|
| 0 | 0.03336 | 0 |
| 1 | 0.88008 | 1.02512 |
| 2 | 2.08248 | 2.12992 |
| 3 | 3.05344 | 3.2596 |
| 4 | 4.06 | 3.93312 |
| 5 | 5.3708 | 4.84984 |
| Slope | 1.063 | 0.974 |
| R2 | 0.997 | 0.994 |

Overlay Range : 0~5nm

As a result of fixing the current layer, the outcome converged to 0. However, the simulation's measurement precision exhibited an error of 0.3 nm, which could be attributed to the measurement process and the influence of the simulation design. The measurement results indicated that the CoG value escalated with each step for the previous layer. This experiment confirmed that the simulation results were calculated accurately, and the adjusted values were reflected in both the current and prior layers accurately. Both the AIM and PGT marks demonstrated high matching values (R2), suggesting that precision is likely to be enhanced compared to conventional marks. This is attributed to the PGT's slope being smaller than that of the AIM, indicating a potential improvement in precision.

### B. AIM vs. PGT Device Test

We fabricated test wafers to experiment with actual equipment, incorporating both AIM and PGT marks into these wafers. The cross-sectional structure of these marks is illustrated in Fig. 11. Measurements were carried out using the Aurotech IBO tool. The test involved repeated measurements of the two marks, each measured ten times. These measurements were conducted at ten different sites on a single wafer, with each site containing two overlay marks.
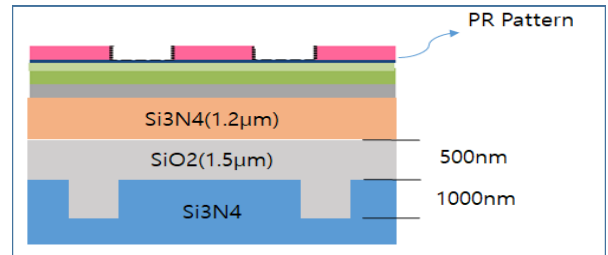


Fig. 11 Cross-sectional structure of the test wafer

The test was performed under the same conditions for both marks. The performance of overlay measurement is typically evaluated based on random error contributions, such as precision and TIS variability, as shown in Table I. In this experiment, we also evaluated based on these metrics [30].

TABLE I
PERFORMANCE EVALUATION (AIM VS. PGT)

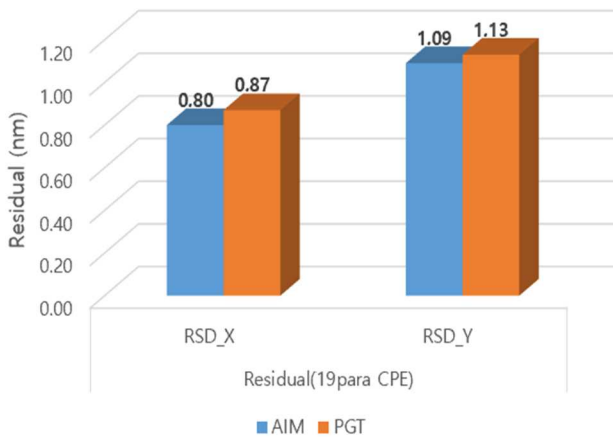| Tool | Mark | Filter | NA | Overlay 3sigma [nm] | | F-Residual 19Para CPE [nm] | | TIS_Mean [nm] | | TIS_3sigma [nm] | | Precision [nm] | | TMU [nm] | | MAM-Time [sec] |
|---|---|---|---|---|---|---|---|---|---|---|---|---|---|---|---|---|
| | | | | X | Y | X | Y | X | Y | X | Y | X | Y | X | Y | |
| Aruos (OL-900n) | AIM | RED | O100 | 4.43 | 3.59 | 0.80 | 1.09 | 0.00 | -0.01 | 0.14 | 0.19 | 0.09 | 0.09 | 0.17 | 0.21 | 0.360 |
| | PGT | RED | O100 | 4.35 | 3.87 | 0.87 | 1.13 | 0.01 | -0.06 | 0.13 | 0.18 | 0.05 | 0.07 | 0.14 | 0.20 | 0.361 |



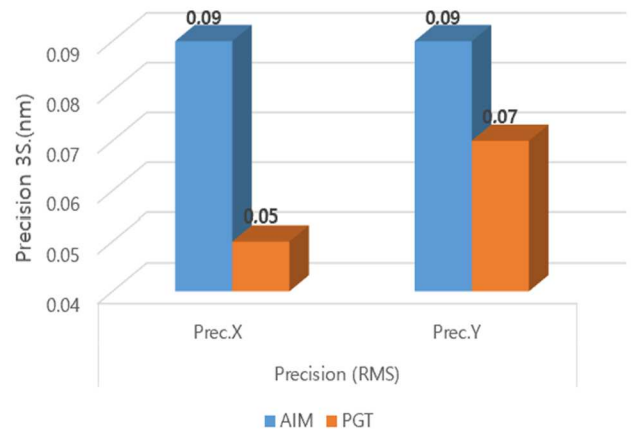Fig. 12 Performance evaluation (AIM vs. PGT): Residual



Fig. 13 Performance evaluation (AIM vs. PGT): Precision

Fig. 12 and Fig. 13 show the performance analysis results of the AIM, the conventional overlay mark, and the PGT, the proposed overlay mark. Overall, they show similar performance, but the PGT outperforms AIM by a factor of 2 in terms of precision. The PGT mark showed an improvement of approximately 17% in total measurement uncertainty (TMU [31]) over the AIM mark. Meanwhile, the final residual was slightly degraded.

## IV. CONCLUSION

This study investigated overlay marks and an overlay measurement method using them. We validated the practical applicability of the proposed PGT method through experimental work. Additionally, we addressed the precision and reliability of overlay measurements by resolving the significant challenge posed by large overlays, a prominent issue with grating patterns, while concurrently enhancing mark performance.

Recently, the demand for minor overlay marks has increased as the size of semiconductor circuit patterns has decreased. This study aimed at addressing the significant overlay problem, which becomes more probable as sizes reduce and at the possibility of incorporating more patterns within the same area. The irregular grating pattern employed in this study effectively designs more minor marks, offering promising prospects for future research on small overlay mark design. In summary, our findings are anticipated to contribute significantly to the overlay mark research field.

## REFERENCES

[1] H. Lee, H. Chang, H. Shin, and O. Choi, "Image-based overlay target design using a grating intersection," Journal of Micro/Nanopatterning, Materials, and Metrology, vol. 21, no. 03, Sep. 2022, doi:10.1117/1.jmm.21.3.034801.

[2] N. Wang, Y. Li, F. Sha, and Y. He, "Sub-nanometer misalignment sensing for lithography with structured illumination," Optics Letters, vol. 47, no. 17, p. 4427, Aug. 2022, doi: 10.1364/ol.468177.

[3] H. Lee et al., "Improved accuracy and robustness for advanced DRAM with tunable multi-wavelength imaging and scatterometry overlay metrology," Metrology, Inspection, and Process Control for Microlithography XXXIII, Mar. 2019, doi: 10.1117/12.2515015.

[4] S. Katz et al., "OPO residuals reduction with imaging metrology color per layer mode," Metrology, Inspection, and Process Control for Microlithography XXXIV, Mar. 2020, doi: 10.1117/12.2541933.

[5] S. Katz et al., "OPO robustness and measurability improvement via extended wavelengths," Metrology, Inspection, and Process Control XXXVII, Apr. 2023, doi: 10.1117/12.2655161.

[6] H. Jin and Y. Qi, "Review of overlay error and controlling methods in alignment system for advanced lithography," Thirteenth International Conference on Information Optics and Photonics (CIOP 2022), Dec. 2022, doi: 10.1117/12.2654908.

[7] H. Ina, T. Matsumoto, K. Sentoku, K. Matsuyama, and K. Katagiri, "New criterion about the topography of W-CMP wafer's alignment mark," Metrology, Inspection, and Process Control for Microlithography XVII, May 2003, doi: 10.1117/12.504579.

[8] T. Nagayama, M. Yasuda, Y. Kanaya, T. Masada, and A. Sugaya, "Advanced alignment optical system for DUV scanner," SPIE Proceedings, May 2004, doi: 10.1117/12.535083.

[9] S. Keij, I. Setija, G. van der Zouw, and E. Ebert, "Advances in phase-grating-based wafer alignment systems," Metrology, Inspection, and Process Control for Microlithography XIX, May 2005, doi:10.1117/12.599090.

[10] B. Menchtchikov et al., "Computational scanner wafer mark alignment," Optical Microlithography XXX, Mar. 2017, doi:10.1117/12.2259750.

[11] C. Messinis et al., "Diffraction-based overlay metrology using angular-multiplexed acquisition of dark-field digital holograms," Optics Express, vol. 28, no. 25, p. 37419, Nov. 2020, doi:10.1364/oe.413020.

[12] H.-C. Hsieh, "Improving the cross-layer misalignment measurement accuracy by pattern-center shift induced error calibration," Optics and Lasers in Engineering, vol. 155, p. 107051, Aug. 2022, doi:10.1016/j.optlaseng.2022.107051.

[13] K. Koga et al., "Improvement of heterodyne alignment technique for x-ray steppers," Journal of Vacuum Science &amp; Technology B: Microelectronics and Nanometer Structures Processing, Measurement, and Phenomena, vol. 11, no. 6, pp. 2179–2182, Nov. 1993, doi:10.1116/1.586452.

[14] T. Shu et al., "Measurement algorithm for wafer alignment based on principal component analysis," Applied Optics, vol. 60, no. 19, p. 5569, Jun. 2021, doi: 10.1364/ao.425767.

[15] L. Zhang et al., "Overlay mark sub structure design to improve the contrast," 2020 International Workshop on Advanced Patterning Solutions (IWAPS), Nov. 2020, doi:10.1109/iwaps51164.2020.9286790.

[16] Z. Liu, E. Hajaj, I. Naot, R. Yohanan, and Y. Grauer, "OPO reduction by novel target design," Metrology, Inspection, and Process Control for Microlithography XXXIV, Mar. 2020, doi: 10.1117/12.2552000.

[17] H.-C. Hsieh, M.-R. Wu, and X.-T. Huang, "Designing Highly Precise Overlay Targets for Asymmetric Sidewall Structures Using Quasi-Periodic Line Widths and Finite-Difference Time-Domain Simulation," Sensors, vol. 23, no. 9, p. 4482, May 2023, doi:10.3390/s23094482.

[18] M. Adel et al., "Optimized Overlay Metrology Marks: Theory and Experiment," IEEE Transactions on Semiconductor Manufacturing, vol. 17, no. 2, pp. 166–179, May 2004, doi: 10.1109/tsm.2004.826955.

[19] J. R. Jordan III, "Alignment mark detection using signed-contrast gradient edge maps," Machine Vision Applications in Character Recognition and Industrial Inspection, Aug. 1992, doi:10.1117/12.130304.

[20] M. Adel et al., "Characterization of overlay mark fidelity," Metrology, Inspection, and Process Control for Microlithography XVII, May 2003, doi: 10.1117/12.483430.

[21] M. Adel et al., "Performance study of new segmented overlay marks for advanced wafer processing," Metrology, Inspection, and Process Control for Microlithography XVII, May 2003, doi:10.1117/12.483477.

[22] J. L. Seligson, M. E. Adel, P. Izikson, V. Levinski, and D. Yaffe, "Target noise in overlay metrology," SPIE Proceedings, May 2004, doi:10.1117/12.534515.

[23] E. Lantz, "Subpixel signal centering and shift measurement using a recursive spectral phase algorithm," Signal Processing, vol. 17, no. 4, pp. 365–372, Aug. 1989, doi: 10.1016/0165-1684(89)90121-7.

[24] S. Pan et al., "Sub-pixel position estimation algorithm based on Gaussian fitting and sampling theorem interpolation for wafer alignment," Applied Optics, vol. 60, no. 31, p. 9607, Oct. 2021, doi:10.1364/ao.437440.

[25] L. H. Chul and W. H. Sung, "Motion Vector Based Overlay Metrology Algorithm for Wafer Alignment," KIPS Transactions on Software and Data Engineering, vol. 12, no. 3, pp. 141-148, 2023. doi:10.3745/KTSDE.2023.12.3.141.

[26] K. Sentoku, T. Matsumoto, and H. Ina, "Novel strategy for wafer-induced shift (WIS)," Optical Microlithography XV, Jul. 2002, doi:10.1117/12.474477.

[27] A. Sugaya, Y. Kanaya, S. Nakajima, T. Nagayama, and N. Shiraishi, "Optical Alignment Optimizations for Reducing Wafer-Induced Shift," Japanese Journal of Applied Physics, vol. 43, no. 11A, pp. 7419–7426, Nov. 2004, doi: 10.1143/jjap.43.7419.

[28] A. J. den Boef, "Optical wafer metrology sensors for process-robust CD and overlay control in semiconductor device manufacturing," Surface Topography: Metrology and Properties, vol. 4, no. 2, p. 023001, Feb. 2016, doi: 10.1088/2051-672x/4/2/023001.

[29] C. W. Wong et al., "Self-referenced and self-calibrated MoiréOVL target design and applications," Metrology, Inspection, and Process Control for Semiconductor Manufacturing XXXV, Feb. 2021, doi:10.1117/12.2583733.

[30] D. Kandel et al., "Overlay accuracy fundamentals," Metrology, Inspection, and Process Control for Microlithography XXVI, Mar. 2012, doi: 10.1117/12.916369.

[31] H. Kim et al., "Effective tool induced shift (eTIS) for determining the total measurement uncertainty (TMU) in overlay metrology," Metrology, Inspection, and Process Control XXXVII, Apr. 2023, doi:10.1117/12.2670420.